Extended Abstracts of the 2002 International Conference on Solid State Devices and Materials, Nagoya, 2002, pp. 414-415

P2-16

Impact Ionization Model Using First Three Moments of Energy Distribution Function

Ting-wei Tang, Qi Cao, and Joonwoo Nam[1]

Department of Electrical and Computer Engineering
University of Massachusetts, Amherst, MA 01003, USA
Phone: 413-545-0763 Fax: 413-545-4611 Email: ttang@ecs.umass.edu,
[1]Compaq Computer Corporation, Shrewsbury, MA 01545, USA

1. Introduction

Hot-carrier related effects may be less problematic for deep submicron MOS devices because of reduction in the drain voltage. However, the non-local effect is greatly enhanced and the conventional local field- or even energy-dependent impact ionization (II) model is no longer adequate for describing the II phenomenon in this regime. It is rather difficult to model an energy distribution function near the drain where there exists an admixture of hot-electrons streaming toward the drain and cold-electrons back diffusing from the drain [1]. Sonoda et al. [2] were the first to seek such analytical model and a recent model of Grasser et al. [3] makes it possible to obtain a result in closed form. This work represents a continued development and improvement of the II model in [2], [3].

2. Distribution Function Model

Our energy distribution function normalized with respect to the carrier concentration n takes the form:

$$f(\varepsilon)/n = (1-\rho)\frac{\exp[-(\varepsilon/a_c)]}{M_0(a_c,1)g_0} + \rho\frac{\exp[-(\varepsilon/a_h)^{b_h}]}{M_0(a_h,b_h)g_0} \tag{1}$$

The first term on the r. h. s. of (1) corresponds to f_{cold} and the second term to f_{hot} in [2]. $M_l(a,b)g_0$ represents the l-order moment of each energy distribution function and can be expressed in terms of Gamma function[3]. Our model differs from [2] in that (i) a_c is not a constant, (ii) $\rho = n_{hot}/n$ is not taken as n_{min}/n, and (iii) $\beta_h = 3\langle\varepsilon^2\rangle_h/5\langle\varepsilon\rangle_h^2$ is not fixed at 0.7744. Instead the parameters ρ, a_c, β_h are carefully modeled in each well defined, distinct region where the II is important.

3. Simulation Results

To test our II model, we simulate three n^+-n-n^+ structures with different length L of the active n-region using the Monte Carlo (MC) particle simulation. Figs. 1-3 show the comparison between the model prediction and the MC energy distribution data at three different locations for L=100nm. We calculate the II generation rate by

$$G_{ii} = \int_{\varepsilon_{th}}^{\infty} P_{ii}(\varepsilon) f(\varepsilon) g(\varepsilon) d\varepsilon \tag{2}$$

using the Keldysh formula $P_{ii}(\varepsilon) = P_0(\varepsilon - \varepsilon_{th})^2/\varepsilon_{th}^2$ with $P_0 = 4.18\times10^{12}\text{s}^{-1}$ and $\varepsilon_{th} = 1.12\text{eV}$ [3]. Figs. 4-6 compare the calculated II rate with the MC result, all using the same II model. The overall agreement is very good. Although the peak electric field occurs at the n-n^+ junction for all three test structures, there is a progressive spatial delay for the peak II rate. Approximately, a spatial delay of 5nm, 10nm, and 13nm from the junction is observed for L = 100nm, 70nm, and 50nm, respectively. In addition, even though the peak electric fields of these test structures are respectively 300kV/cm, 358kV/cm, and 410kV/cm, their peak II rates are $1.2\times10^{11}\text{s}^{-1}$, $8.9\times10^{10}\text{s}^{-1}$, and $7.1\times10^{10}\text{s}^{-1}$, respectively. In the deep submicron regime, the inelastic mean-free-path (30nm ~ 100nm) becomes comparable to the length of device active region, resulting in a strong non-local effect of the II.

4. Conclusion

We have further improved the accuracy of the original II model of Sonoda et al. [2] by carefully modeling the parameters ρ, a_c, and β_h in each distinct II region. Because only three moments are utilized, the model has its own limitations. Nevertheless, if the model parameters are carefully chosen, it can describe the shape of energy distribution function fairly accurately, at least for the purpose of calculating the II rate. Following the approach of [4], the model can also be extended to 2-D simulation of substrate currents in deep submicron MOSFETs.

References:

[1] T. J. Bordelon, V. M. Jr. Agostinelli, X.-L. Wang, C. M. Maziar, and A. F. Tasch, Electron Lett. **28**, 1173 (1992)

[2] K. Sonoda, S. T. Dunham, M. Yamaji, K. Taniguchi, and C. Hamaguchi, Jpn. J. Appl. Phys. **35**, 818 (1996)

[3] T. Grasser, H. Kosina, and S. Selberherr, SISPAD, Athens, Greece, pp. 46-49 (2001)

[4] K. Sonoda, M. Yamaji, K. Taniguchi, and C. Hamaguchi, J. Appl. Phys. **80**, 5444 (1996)

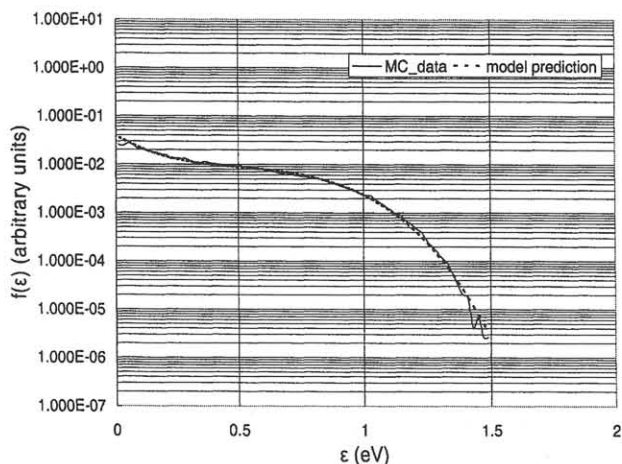

Fig. 1 Comparison of energy distribution function between the MC data and the model prediction for L=100nm at $<\varepsilon^2>=<\varepsilon^2>_{max}$ (chosen as $x=x_0$).

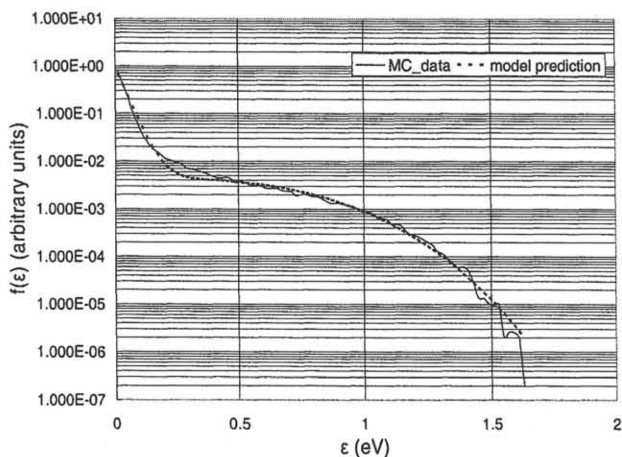

Fig. 2 Comparison of energy distribution function between the MC data and the model prediction for L=100nm at $x=x_0+10$ nm.

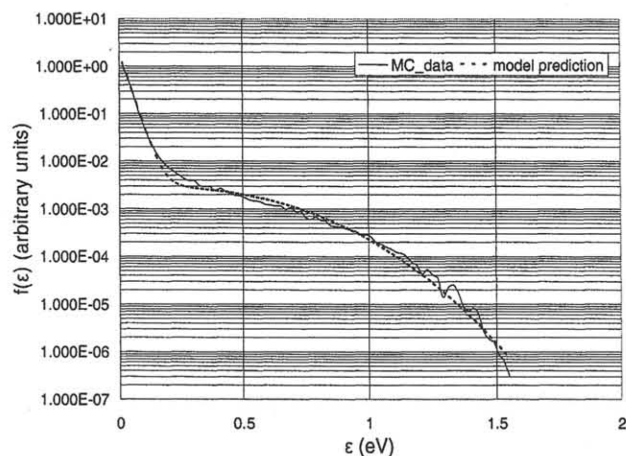

Fig. 3 Comparison of energy distribution function between the MC data and the model prediction for L=100nm at $x=x_0+20$ nm.

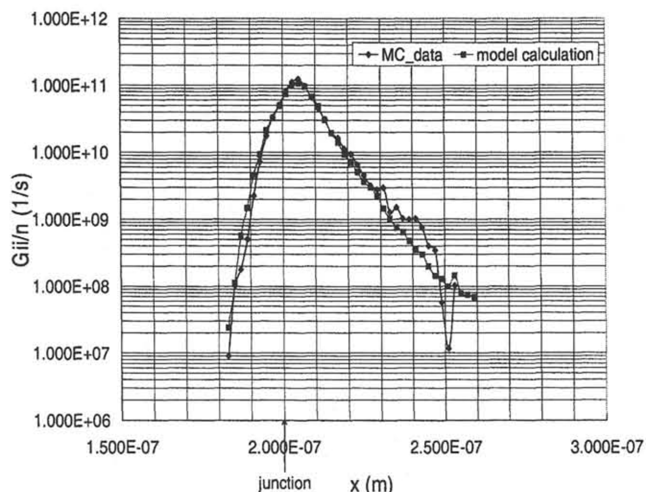

Fig. 4 Comparison of II rate between the MC result and the model calculation for L=100nm.

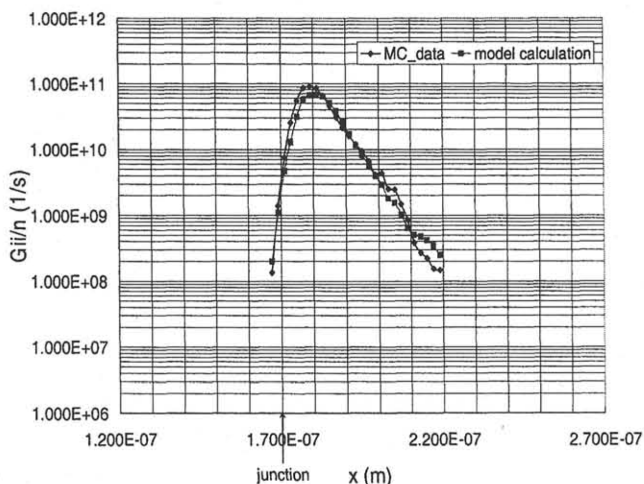

Fig. 5 Comparison of II rate between the MC result and the model calculation for L=70nm.

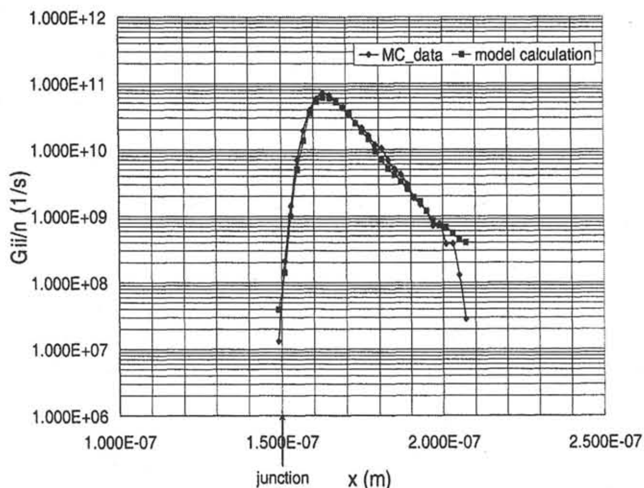

Fig. 6 Comparison of II rate between the MC result and the model calculation for L=50nm.